Final Technical Report

DOE Grant Number: **DE-FG02-07ER46467**

Recipient: **University of Washington**

Project Title: **Molecular and Nanoscale Engineering of High Efficiency Excitonic Solar Cells**

DOE/Office of Science Program Office: **Basic Energy Sciences (BES)**

DOE/Office of Science Program Manager: **Dr. Michael S. Sennett**

Research Area: **Materials Chemistry**

Principal Investigator: **Samson A. Jenekhe**

Co-Principal Investigators: **David S. Ginger and Guozhong Cao**

Period of Performance: **09/01/2007 to 09/30/2014**
Date: **January 15, 2016**

1. Executive Summary

We combined the synthesis of new polymers and organic-inorganic hybrid materials with new experimental characterization tools to investigate bulk heterojunction (BHJ) polymer solar cells and hybrid organic-inorganic solar cells during the 2007-2010 period (phase I) of this project. We showed that the bulk morphology of polymer/fullerene blend solar cells could be controlled by using either self-assembled polymer semiconductor nanowires or diblock poly(3-alkylthiophenes) as the light-absorbing and hole transport component. We developed new characterization tools in-house, including photoinduced absorption (PIA) spectroscopy, time-resolved electrostatic force microscopy (TR-EFM) and conductive and photoconductive atomic force microscopy (c-AFM and pc-AFM), and used them to investigate charge transfer and recombination dynamics in polymer/fullerene BHJ solar cells, hybrid polymer-nanocrystal (PbSe) devices, and dye-sensitized solar cells (DSSCs); we thus showed in detail how the bulk photovoltaic properties are connected to the nanoscale structure of the BHJ polymer solar cells. We created various oxide semiconductor (ZnO, TiO_2) nanostructures by solution processing routes, including hierarchical aggregates and nanorods/nanotubes, and showed that the nanostructured photoanodes resulted in substantially enhanced light-harvesting and charge transport, leading to enhanced power conversion efficiency of dye-sensitized solar cells.

Our research efforts during the 2011-2014 period (phase II) focused on using tailored new organic and inorganic materials in combination with device measurements and optical spectroscopy to understand the fundamental factors, such as energy level offsets, relative dielectric constants, interfacial chemistry, and morphology, that control relative branching ratios between geminate recombination and free carrier generation at various model donor/acceptor interfaces. Among the new materials we synthesized were a series of p-type (donor) thiazolothiazole-based conjugated polymers with different *type* (alkyl, alkoxy, aryl), *size* , *topology* (linear, branched) and *distribution* (uniform, alternating, random) of side chains, leading to the finding that such *side chain engineering* can have a huge impact on and thus provide a means to control the morphology (crystallinity, π-stacking orientations), charge transport and photovoltaic properties of BHJ polymer solar cells. Another series of new polymer semiconductors proved to be excellent hosts that enabled observation of efficient charge transfer to small bandgap PbS quantum dots in polymer/quantum dot blend devices. Using the same polymer/PbS blend system we also established the relative contributions of forward electron transfer and back hole transfer to photocurrent generation in

hybrid polymer/quantum dot solar cells. In the case of polymer/fullerene BHJ solar cells, we found that photoinduced hole transfer becomes suppressed with diminishing driving force while electron transfer remains active, resulting in diminished power conversion efficiency. To harvest more of the solar spectrum and increase the open circuit voltage (V_{oc}) of organic photovoltaic devices, we explored new organic acceptors and discovered two new classes of non-fullerene acceptors – small molecules and polymeric – that had enhanced V_{oc} while other photovoltaic properties were either comparable or superior to conventional fullerene-based acceptors.

2. Comparison of Accomplishments with Project Goals and Objectives During 2007-2014.

The main objectives of the integrated research project during the 2007-2010 period (phase I) were: (1) to develop new polymer or hybrid organic-inorganic materials, nanostructured conductive/semiconductive oxides as charge-collecting electrodes, and explore them in device architectures that will enable realization of high efficiency polymer and hybrid organic-inorganic photovoltaic cells; (2) to develop test beds consisting of device structures, fabrication methods, and standardized evaluation for the consistent and realistic appraisal of organic and hybrid organic-inorganic photovoltaic cells; and (3) to use these new materials and methods to achieve both improved device efficiency, and advance our fundamental understanding of the physical/chemical processes and dynamics underlying the harvesting of photons and their efficient conversion into electrical power in organic and organic-inorganic solar cells.

All of these objectives were substantially achieved by exploring various new concepts of materials, device architectures, and experimental characterization tools for organic and hybrid organic-inorganic photovoltaic cells at the molecular and nanoscales. Specific accomplishments are exemplified in the brief Executive Summary (*Section 1*), in the following *Section 3*, and detailed in the 90 published journal papers[1-90] that acknowledged this grant and are listed below in *Section 4*. New polymers and nanostructed materials developed in pursuit of objective 1 include high molecular weight regioregular poly(3-alkylthiophenes) that controllably self-assembled into 10-30 nm crystalline nanowires as well as the diblock copoly(3-alkylthiophenes) that microphase separate into light-absorbing and hole-conducting nanostructured thin films.[2,3,10,19,20,31,32] Accomplishments relative to objective 2 include the development of in-house characterization tools such as photoinduced absorption (PIA) spectroscopy, time-resolved electrostatic force microscopy (TR-EFM) and conductive and photoconductive atomic force microscopy (c-AFM and pc-AFM), and their successful use to investigate longstanding challenges in charge transfer and recombination dynamics in polymer/fullerene BHJ solar cells,[15,22,31] hybrid polymer-nanocrystal (PbSe) devices,[13,14,24] and dye-sensitized solar cells (DSSCs). Finally, we advanced organic photovoltaic (OPV) device efficiency and fundamental understanding envisioned in objective 3 in many ways,[4-6,12] including observation of enhanced power conversion efficiency, light harvesting and charge transport in dye-sensitized solar cells composed of our designed nanostructured ZnO and TiO_2 photoanodes.[26-30,34,35]

During the 2011-2014 project funding period (phase II), we aimed to harvest more of the solar spectrum while generating larger cell voltages by uncovering the fundamental factors such as energy level offsets, relative dielectric constants, interfacial chemistry, and morphology that control relative branching ratios between geminate recombination and free carrier generation at a range of model donor/acceptor interfaces by coupling tailored materials design of both organic and inorganic materials closely with device measurements and optical spectroscopy. Our studies sought to identify the design rules and fundamental performance limits for new organic and hybrid organic/inorganic photovoltaic materials by pursuing the following specific objectives: (4) develop new p-type polymers with tailored energy level offsets and different morphologies (e.g. π–stacking orientation, crystallinity) to systematically explore the effects of energetics and morphology on recombination loss in polymer/fullerene systems; (5) design and study new hybrid inorganic quantum dot/polymer combinations for extending the response of solution-processable solar cell materials into the near and mid-IR, while exploring the role of acceptor dielectric constant and surface chemistry; (6) manipulate the surface chemistry and facets of ZnO nanostructures towards studies of effects of dielectric constant and morphology on charge injection rate and surface recombination rate in organic/inorganic hybrid systems; (7) explore new n-type polymers with a range of

energy levels, optical bandgaps and carrier mobilities to enable investigation of effects of energetics and morphology on device performance and recombination loss in polymer/polymer bulk heterojunction (BHJ) solar cells for comparison with fullerene acceptors; and (8) use test beds of experimental tools to probe and quantify the performance limits and loss mechanisms in BHJ solar cells based on various model donor/acceptor pairs produced in this project.

These objectives of the 2011-2014 project period were also substantially achieved as exemplified in the brief Executive Summary (*Section 1*), in the following *Section 3*, and detailed in the over 50 published journal papers[36-90] that acknowledged this grant and listed below in *Section 4*. In pursuit of objective 4, we designed and synthesized a series of new p-type (donor) thiazolothiazole-based semiconducting polymers with suitable side chains that enabled improved control of the morphology (e.g. face-on *versus* edge-on molecular packing) and enhanced photovoltaic performance of polymer/fullerene-PCBM blend solar cells.[40,41,57,58] One of these thiazolothiazole-dithienosilole copolymers, PSEHTT, first reported by our group,[41] has proved to be a high performance OPV material, and is now also widely studied by many other laboratories. Studies directed toward objective 5 resulted in a major success in reporting the first examples of efficient BHJ solar cells utilizing IR absorbing PbS quantum dots and a series of new conjugated polymers. In contrast to prior failures in the literature to observe efficient charge transfer in many quantum dot/polymer BHJ devices, by using a new polymer host synthesized in this project, poly(2,3-didecyl-quinoxaline-5,8-diyl-*alt*-*N*-octyldithieno[3,2-*b*:2',3'-*d*]pyrrole) (PDTPQx), we successfully observed the then record efficient quantum dot (PbS)/polymer (PDTPQx) BHJ solar cells. In pursuit of objective 8, we obtained direct spectroscopic evidence of photoinduced hole transfer from PbS to a semiconducting polymer at the inorganic/organic interfaces in hybrid photovoltaics and also established the relative contributions of forward electron transfer and back hole transfer to photocurrent generation in hybrid polymer/quantum dot solar cells. [53,69,70,86,87] We successfully exploited our team's expertise in metal oxide semiconductor chemistry to create nanostructured ZnO andTiO_2 films for inverted polymer solar cells with enhanced performance and stability as envisioned in our project objective 6. [65,67,88,89] Our studies in pursuit of objective 7 explored new electron acceptor materials, which are long sought to overcome the small photovoltage, high cost, poor photochemical stability, and other limitations of fullerene-based organic photovoltaics. We discovered two new classes of non-fullerene acceptors – small molecules[82] and polymeric[72,83] – that had enhanced V_{oc} while other photovoltaic properties were either comparable or superior to conventional fullerene-based acceptors such as the benchmark [6,6]-phenyl-C71-butyric acid methyl ester ($PC_{71}BM$). We have reported a design strategy that has produced the novel multi-chromophoric, large size, non-planar three-dimensional (3D) organic molecule, DBFI-T, whose π-conjugated framework occupies space comparable to an aggregate of 9 [C60]-fullerene molecules. [82]

Further details of the research accomplishments and technical results achieved during the entire 2007-2014 funding period have been summarized in the 90 published journal articles[1-90] and some major results are highlighted below in *Section 3*.

3. Summary of Activities and Results for the 2007-2014 Project Performance Period.

We combined the synthesis of new polymers and organic-inorganic hybrid materials with new experimental characterization tools to investigate bulk heterojunction (BHJ) polymer solar cells and hybrid organic-inorganic solar cells. Among the major accomplishments during the 2007-2010 period of this collaborative project are the following. Thirty-five (35) journal papers were published.[1-35] We highlight below several results; details are in the cited publications. We have discovered that self-assembled conjugated polymer nanowires (NWs) are excellent model systems for investigation of charge and exciton transport while also of use for the construction of efficient BHJ solar cells.[2,3,22,31] We have demonstrated how photoconductive AFM (pcAFM) can be used to image vertical morphology in BHJ solar cells, allowing understanding of the limits of photocurrent and photovoltaic efficiency in BHJ devices based on fullerene and polymer NWs.[22,24,31] We have discovered that diblock copolymers as donors in BHJ solar cells lead to factors of 2–9 times enhanced device efficiencies and enhanced charge transport compared to the parent homopolymers.[32] Our spectroscopic studies have led to an understanding of why conventional bulk heterojunction devices with IR-absorbing quantum dots exhibit poor performance.[14] Coupled materials design and spectroscopic studies have led to discovery of new materials enabling the first ever demonstration of viable bulk-heterojunction polymer/quantum dot devices operating in the infrared.[24] Our research has also advanced the fabrication of nanostructured electrodes of n-type oxide semiconductors including nanotube arrays of ZnO and TiO_2 on FTO and ITO substrates and submicron-sized aggregates of ZnO and TiO_2 nanocrystallites or nanotubes for both dye-sensitized solar cells (DSCs) and hybrid organic/inorganic solar cells.[4-6,8,26-30,34,35] We have discovered the first high-mobility ambipolar charge transport in a polymer semiconductor, suggesting novel approaches to organic electronic devices and circuits.[21] We have synthesized a new class of thiazolothiazole-based low bandgap copolymer semiconductors[40,41] and found that they combine high carrier mobility with high bulk heterojunction photovoltaic efficiency, one of only four polymers reported to have a power conversion efficiency exceeding 5 % at the time. Major results achieved in the entire 2007-2014 project period are briefly highlighted below in *Sections 3.1–3.14*.

Among the major accomplishments during the 2011-2014 project period are the following. Fifty-five (55) journal papers have been published.[36-90] Below we highlight several results; the scientific and technical details are to be found in the appended list of publications. By combining our team's expertise in materials synthesis and optical spectroscopy, we advanced understanding of the driving force for charge transfer at donor/acceptor interfaces in bulk heterojunction (BHJ) solar cells.[71] We reported the first examples of efficient BHJ solar cells utilizing IR absorbing PbS quantum dots and a series of new conjugated polymers.[24,86,87] We have found that the type, size, topology, and distribution of side chains on a conjugated polymer can have a large impact on charge photogeneration and power conversion efficiency, providing new insights for the design of next generation materials.[57,58,60,85] We have obtained direct spectroscopic evidence of photoinduced hole transfer from PbS to a semiconducting polymer at the inorganic/organic interfaces in hybrid photovoltaics.[86] We have found that an electrospray method can be used to synthesize TiO_2 nanoparticles and their aggregates as efficient photoelectrodes for dye-sensitized solar cells (DSCs). We have synthesized a series of oligothiophene-functionalized naphthalene diimides and found that they are very promising non-fullerene organic electron acceptors for BHJ solar cells.[36,39,55] We discovered the first example of a small bandgap donor-acceptor copolymer that in BHJ blends with indene-C_{60} bisadduct (ICBA) results in 40-50% enhancement in V_{oc} (0.9 V) and photovoltaic efficiency (5.4%) compared to PCBM-based devices.[57] We have exploited our team's expertise in metal oxide synthesis to create nanostructured TiO_2 films for inverted polymer solar cells with enhanced stability.[65,67,88,89] New electron acceptor materials are long sought to overcome the small photovoltage, high cost, poor photochemical stability, and other limitations of fullerene-based organic photovoltaics. However, all known non-fullerene acceptors have so far shown inferior photovoltaic properties compared to fullerene benchmark [6,6]-phenyl-C60-butyric acid methyl ester ($PC_{60}BM$). We have reported a design strategy that has produced a novel multi-chromophoric, large size, non-planar three-dimensional (3D) organic molecule, DBFI-T, whose π-conjugated framework occupies space comparable to an aggregate of 9

[C60]-fullerene molecules.[82] Comparative studies of DBFI-T with its planar monomeric analogue (BFI-P2) and PC60BM in bulk heterojunction (BHJ) solar cells, by using a common thiazolothiazoledithienylsilole copolymer donor (PSEHTT), showed that DBFI-T has superior charge photogeneration and photovoltaic properties; PSEHTT:DBFI-T solar cells combined a high short-circuit current (10.14 mA/cm^2) with a high open circuit voltage (0.86 V) to give a power conversion efficiency of 5.0%.

Some of major results and accomplishments achieved during the entire 2007-2014 funding period of the BES-supported project are briefly highlighted below in sections 3.1–3.14.

3.1. Controlling Morphology of Bulk Heterojunction Solar Cells via Self-Assembled Polymer Nanowires. We have discovered that self-assembled polymer semiconductor nanowires (NWs), exemplified by poly(3-butylthiophene) NWs (P3BT-nw), provide a promising approach to efficient bulk heterojunction (BHJ) solar cells.[2,3] In this approach, the polymer NWs function as the donor component and primary absorber in the BHJ devices, providing a means to rationally control the nanoscale morphology.[2,3] We have systematically studied the film morphology, charge transport and photovoltaic properties of P3BT-nw/fullerene nanocomposite films.[31] The charge transport properties of the films were characterized in both bulk field effect transistor and space charge limited current and at the nanoscale. The latter measurements, including conductive and photoconductive Atomic Force Microscopy (cAFM and pcAFM) imaging (**Fig. 1**) were performed by the **Ginger** group. We found that annealing a dry film (long drying time) caused diffusion and aggregation of the fullerene while the polymer NWs remained intact. In this case, high hole mobility along the nanowires was observed, resulting in efficient exciton generation, dissociation, and charge transport, and thus high current density.[70] A power conversion efficiency of 3.5% was achieved from P3BT-nw:$PC_{71}BM$ devices annealed wet, after a short drying time, with J_{SC} = 9.2 mA/cm^2, V_{OC} = 0.60, and *FF* = 0.61. The best photovoltaic performance is realized in a device structure which maintains the interpenetrating network of nanowires (high current density), but avoids the device bridging, and the recombination and shunt losses associated with it (high open-circuit voltage).[31]

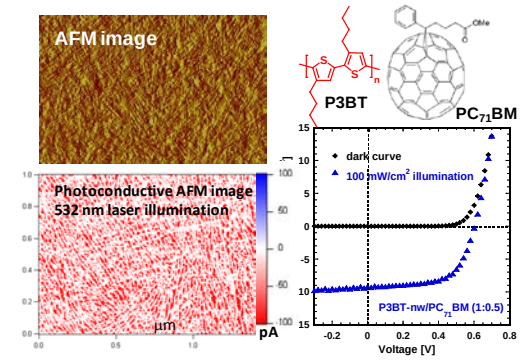

Fig. 1. Tapping mode phase AFM image; photoconductive AFM image and J-V curves of P3BT-nw:$PC_{71}BM$ solar cells.

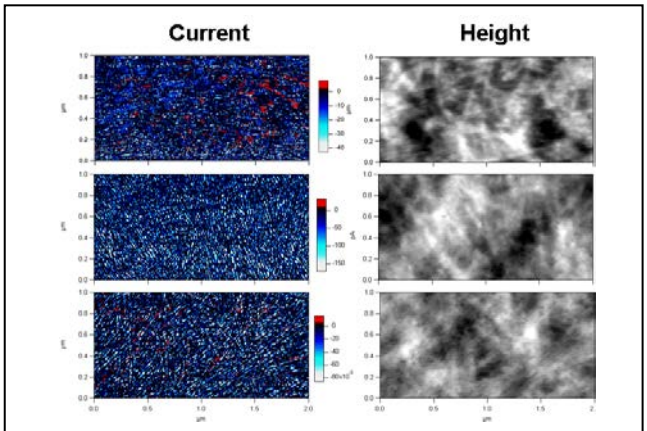

Fig. 2. Simultaneously acquired topography (right) and photocurrent (left) images of a P3BT:PCBM solar cell acquired using pcAFM. The photocurrent image shows enhanced photocurrents associated with the P3BT nanowires.

A major theme of our original proposed work is the use of novel scanning probe microscopy tools being developed in the **Ginger** lab to study photocurrent distributions in nanostructured solar cells prepared from materials synthesized in the **Jenekhe** and **Cao** labs. Over the past two years we have systematically applied photoconductive AFM (pc-AFM) to study the photocurrent distribution in the P3BT-nw:PCBM solar cells produced under this grant (**Fig. 2**).[31] The results show direct correlations between the evolution of the nanowire network and the device performance. For instance, although the nanowires enhance photocurrent collection, when we observe conductive nanowires that penetrate the entire film thickness we also observe lower open circuit voltages due to wires

introducing a shunt resistance. In addition, the changing local V_{OC} measured via pc-AFM provides evidence of changes in vertical film composition upon annealing.[31]

3.2 Nanostructured Oxide Electrodes for Dye-sensitized Solar Cells. Dye-sensitized solar cells (DSCs) are a type of photoelectrochemical photovoltaic device with low cost and decent power conversion efficiency (~10%). Traditional DSCs consist of a photoanode made of TiO_2 nanoparticles sensitized by ruthenium-based dyes, such as commercially available N3, N719, and Black dye. Due to the limitation of electron transport in a nanoparticle film, the photoanode film of a traditional DSC typically cannot be thicker than 15 μm, which however leads to an insufficient optical absorption diminishing the solar cell power conversion efficiency. The **Cao** group developed a nanocrystallite aggregate structure which consists of nano-sized crystallites of oxide forming a micro-sized spherical aggregates (**Fig. 3a**).[4,5] On one hand, the feature of the aggregates consisting of nano-sized crystallites makes them possess internal surface area as large as that of nanoparticles, so when being used for the photoanode of DSCs, the aggregates can provide sufficient surface area for dye adsorption. On the other hand, in view of the micro size of aggregates, which are comparable with the wavelengths of visible light, the aggregates can scatter the incident light very effectively, resulting in an extension of the distance of light traveling within the photoanode film and thus an enhancement of optical absorption due to the increased probability for photons to interact with the dye molecules adsorbed on the nanocrystallites of oxide. In the case of ZnO, such a method has resulted in the solar cell power conversion efficiency increasing more than doubly (**Fig. 3b**).[4,5] Through the fabrication of aggregates with different size, it was found that the aggregates with the size closest to the wavelengths of incident light and with a broad size distribution gave rise to the highest power conversion efficiency, proving that light scattering generated by the aggregates contributes to the optical absorption of the photoanode film and thereby benefits the power conversion efficiency of the solar cell.[5] Like the use of nanostructures for anti-reflection, the use of nanocrystallite aggregates for light scattering we have developed is another representative example demonstrating that solar cell performance can be improved through the use of nanostructured materials that generate unique optical effects enhancing the light harvest of solar cells. This work has opened up a new research direction in the fields of dye and quantum dot sensitized solar cells, and has resulted in the publications of three highly cited papers in Adv. Mater.,[12] Nano Today,[47] and Physical Chemistry Chemical Physics.[56]

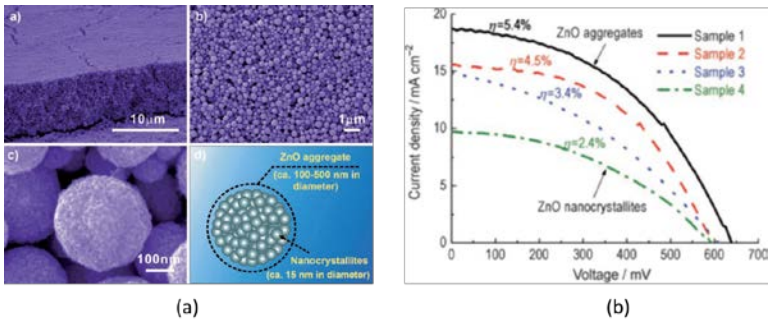

(a) (b)

Fig. 3. ZnO nanocrystallite aggregates for the enhancement of dye-sensitized solar cell performance. (a) SEM images and a schematic drawing of ZnO nanocrystallite aggregates, and (b) Efficiency increase as the ZnO structure evolving from dispersed nanocrystallites to nanocrystallite aggregates.

3.3 Explaining the early failures seen in the literature when trying to make bulk heterojunction solar cells using low-bandgap quantum dot/polymer composites. Seeking to understand why so many polymer/quantum dot blends were failing to live up to expectations, we decided to examine the basic charge transfer processes at a range of polymer/quantum dot interfaces. We used photoluminescence (PL) quenching and photoinduced absorption spectroscopy to study charge transfer in bulk heterojunction blends of PbSe quantum dots with the model semiconducting polymers poly-3-hexylthiophene (P3HT) and poly[2-methoxy-5-(3′,7′-dimethyloctyloxy)-*para*-phenylene vinylene] (MDMO-PPV). We compared these photoinduced absorption spectra from the PbSe blends with spectra from similar blends of the same polymers with phenyl-C_{61}-butyric acid methyl ester (PCBM) and blends with CdSe quantum dots – both electron acceptors that were known to yield much higher efficiency photovoltaic devices. We found that the MDMO-PPV PL was quenched, and the PL lifetime was shortened upon addition of PbSe quantum dots. Unexpectedly, we found that the PL of the P3HT was relatively unaffected upon blending. We also found that the PbSe quantum dot blends with both polymers gave very little polaronic signal in the photoinduced absorption spectra (**Fig. 4**), suggesting that few, if any, long-lived charges are being produced by photoinduced charge transfer. These results provided a clear explanation for why PbSe/conjugated polymer blends were not working as others had expected, and pointed a clear path towards resolving this problem.[14]

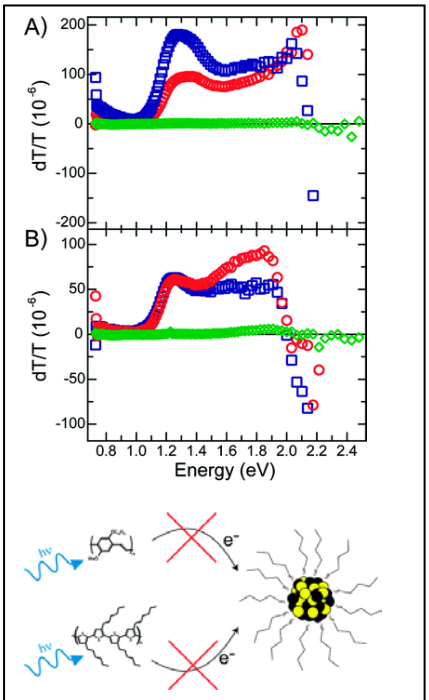

Fig.4. Explaining the early failures of IR absorbing quantum dot/polymer blends. X-Channel PIA spectra for (A) PPV and (B) P3HT blends with PCBM (red circles), CdSe QDs (blue squares), and PbSe QDs (green diamonds).

3.4 Broadband Absorbing Bulk Heterojunction Photovoltaics Using Low-Bandgap Solution-Processed Quantum Dots. We reported the *first ever* examples of efficient (~50X higher quantum efficiencies compared to previous examples) bulk heterojunction (BHJ) solar cells that use low bandgap quantum dots as electron acceptors.[24] We achieved this result through a basic science understanding by combining our team's expertise in polymer chemistry, quantum dot chemistry, and optical spectroscopy. Building on our earlier results that demonstrated that previous attempts to produce organic/lead chalcogenide bulk heterojunctions had failed due to a lack of photoinduced charge transfer, we used photoinduced absorption (PIA) spectroscopy to screen for favorable charge transfer in energetically-promising blends of PbS quantum dots (synthesized in the **Ginger** group) with a variety of new conjugated polymers (synthesized in the **Jenekhe** group) (**Fig. 5**). We found that blends of PbS quantum dots with the poly(2,3-didecyl-quinoxaline-5,8-diyl-*alt*-*N*-octyldithieno[3,2-*b*:2',3'-*d*]pyrrole) (**PDTPQx**), produced significantly more photogenerated charges than blends of PbS with the other donor-acceptor copolymers or with traditionally studied polymers like poly[2-methoxy-5-(3',7'-dimethyloctyloxy)-para-phenylene vinylene] (MDMO-PPV) and poly-3-

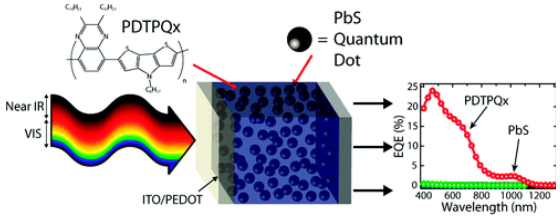

Fig. 5. We reported the first ever examples of moderately efficient bulk heterojunction solar cells comprising blends of a conjugated polymer with lead chalcogenide quantum dots based on the polymer poly(2,3-didecyl-quinoxaline-5,8-diyl-**alt**-**N**-octyldithieno[3,2-*b*:2',3'-*d*]pyrrole). This result was enabled by understanding that the failure of previous materials combinations was due to a lack of long-lived charge transfer at the polymer/quantum dot interface. These blends gave photocurrent response across the visible and into the near infrared.

hexylthiophene (P3HT). Photovoltaic devices made with PDTPQx/PbS blends exhibit power conversion efficiencies ~50 times larger than previously reported BHJ blends made with IR-absorbing quantum dots.

3.5 Suppression of Hole Transfer with Diminished Driving Force in Polymer/Fullerene Blends. We have demonstrated that the reduced photocurrent yield in a derivatized fullerene blend was partly due to the suppression of hole transfer due to reduced driving force.[71] This work addressed a key fundamental question of the driving force needed to support exciton dissociation and subsequent charge escape from the donor/acceptor interface in polymer fullerene blends, focusing on the less-studied topic of *hole back transfer* from the fullerene (**Fig. 6**). We also showed that a state energy picture of the charge transfer driving force could better predict photocurrent generation than a HOMO/LUMO offset picture. To accomplish this we studied photoinduced charge transfer and device performance in blends of several fullerene acceptors ($PC_{71}BM$, $PC_{61}BM$ and the indene-C_{60} *bis*-adduct $IC_{60}BA$) with a polymer donor with a large oxidation potential, poly[(4,8-bis(2-hexyldecyl)oxy)benzo[1,2-b:4,5-b']dithiophene)-2,6-diyl-alt-(2,5-bis(3-dodecylthiophen-2-yl)benzo[1,2-d;4,5-d']bisthiazole)] (PBTHDDT) (prepared in the **Jenekhe** lab).

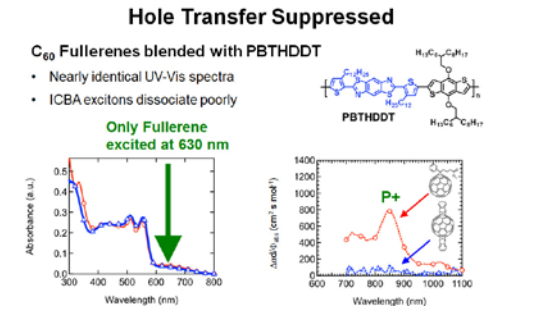

Fig. 6. We confirmed that the reduced EQE of a polymer/ICBA blend was at least in part due to lack of hole transfer from ICBA excitons to the polymer. Suppressed hole transfer from fullerene excitons is an important consideration for materials design when relying heavily on fullerene absorption and in cases where energy transfer from the donor may generate fullerene excitons.

We found that hole transfer from $IC_{60}BA$ excitons to the host polymer is turned off, while electron transfer from the polymer excitons to the $IC_{60}BA$ remains active. On the other hand a relatively small driving force of ca. 70 meV (measured from the state energies) appears to sustain photoinduced hole transfer from $PC_{61}BM$. Power conversion efficiency improves from 1.52% in $IC_{60}BA$-based solar cells to 3.75% in $PC_{71}BM$-based devices. Photoinduced absorption (PIA) of PBTHDDT:fullerene blends performed in the **Ginger** lab demonstrated that exciting the donor leads to long-lived positive polarons on the polymer and negative polarons on the fullerene in all three blends. Selective excitation of $PC_{71}BM$ or $PC_{61}BM$ blends also generates long-lived polarons. In contrast, no discernible PIA features were observed when selectively exciting the $IC_{60}BA$ component of a blend, demonstrating that hole transfer from the $IC_{60}BA$ excitons to the polymer was inefficient. Suppressed hole transfer from fullerene excitons is a potentially important consideration for materials design and device engineering of organic solar cells relying heavily on fullerene absorption and in cases where energy transfer from the donor may generate fullerene excitons.

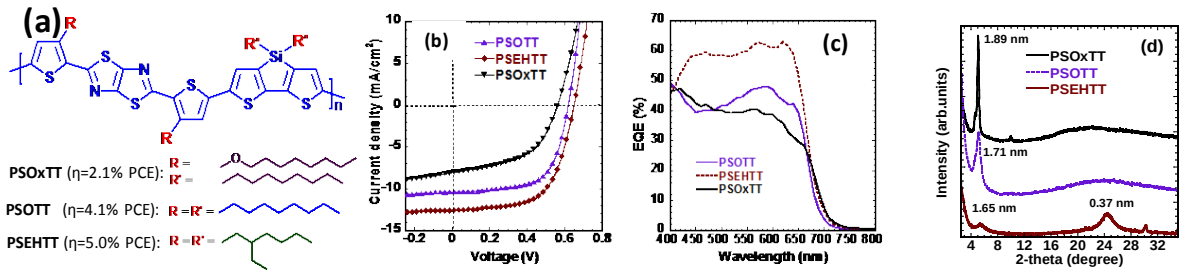

Fig. 7. (a) Chemical structures of new donor-acceptor copolymers, PSOxTT, PSOTT, and PSEHTT. (b) The current density ─ voltage characteristics of PSOTT:$PC_{71}BM$ (1:2), PSEHTT:$PC_{71}BM$ (1:2), and PSOxTT:$PC_{71}BM$ (1:2) solar cells. (c) EQE spectra of the solar cells, measured on devices with an active area of 9 mm^2. (d) Optical absorption spectra of PSOTT/$PC_{71}BM$ (1:2) and PSEHTT:$PC_{71}BM$ (1:2) thin films; (d) X-ray diffraction (XRD) spectra of drop-cast films of PSOxTT, PSOTT and PSEHTT on ITO/PEDOT substrate after annealing at 180 ^oC.

3.6 Effects of Side Chains on Charge Photogeneration and Efficiency of Polymer Solar Cells. We

have found that for the same conjugated polymer backbone the *type* (alkyl, alkoxy, aryl), *size* , *topology* (linear, branched) and *distribution* (uniform, alternating, random) of side chains can have a large impact on the morphology (crystallinity, π -stacking orientations), charge transport and photovoltaic properties of BHJ solar cells comprising the conjugated polymer semiconductors as donor and fullerene acceptor.[41]

These findings are exemplified by the series of thiazolothiazole-dithienosilole based donor-acceptor copolymers with different side chains (**Fig. 7a**). The current density-voltage (*J –V*) curves and the external quantum efficiency (EQE) spectra of the solar cells were showed in (**Fig. 7b & 7c**). Although the copolymer semiconductors showed high hole mobility (0.01-0.12 cm^2/Vs) and similar HOMO/LUMO energy levels, changing the side chains from linear-octyloxy to linear octyl, to branched ethylhexyl resulted in the average power conversion efficiency (PCE) improving from 2.1% in PSOxTT to 4.1% in PSOTT to 5.0% in PSEHTT, respectively. The PSEHTT:$PC_{71}BM$ device also showed the highest photoconversion efficiency with a monochromatic EQE around 60% over the 450–650 wavelength range. The charge photogeneration rate as measured by transient absorption spectroscopy was found to be in the same proportion as the photovoltaic efficiency: PSETHH>PSOTT>PSOxTT. The observed dependence of the charge photogeneration and power conversion efficiency on the side chains of these copolymers was found to originate from the morphology and molecular orientation of the polymer backbone in the blend films. X-ray diffraction studies (**Fig. 7d**) showed that PSOxTT and PSOTT chains were packed edge-on to the substrate whereas PSEHTT chains were oriented face-on to the substrate.

3.7 Measurement of Back-Hole Transfer at Hybrid Organic/Inorganic Interfaces. Polymer/quantum dot bulk heterojunctions have been known since the 1990s. However, the mechanism of photocurrent generation remains an open question in many systems. Whereas our previous work has shown that photoexcitation of the polymer clearly results in photoinduced charge transfer leaving a positive polaron on the polymer, it has been difficult to ascertain if photoexcitation of the quantum dots leads to a similar final state. We have now produced direct spectroscopic evidence that photoinduced hole transfer takes place from PbS quantum dots to a semiconducting polymer host.[69]

We obtained this result using our workhorse photoinduced absorption (PIA) spectroscopy experiment to study blends of the PDTPQx polymer (prepared by **Jenekhe**) with PbS quantum dots (made by **Ginger**). The resulting PIA spectra (**Fig. 8**) show a clear spectral fingerprint of an identical polymer polaron resulting from either direct visible excitation of the polymer, or selective infrared excitation of the PbS quantum dots.

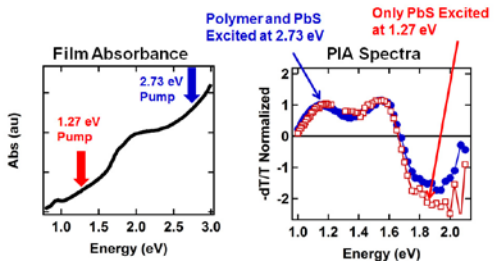

Fig. 8. We have obtained direct spectroscopic confirmation of hole generation on the polymer host following selective photoexcitation of the inorganic PbS quantum dot acceptors. This confirms that hole back transfer from PbS to the polymer takes place, meaning that the IR photocurrent contains a strong contribution from a bulk heterojunction-like photocurrent generation mechanism in this blend.

3.8 Quantum Dot-Sensitized Solar Cells. Quantum dots can function as sensitizers for efficient light harvesting in solar cells and have the potential to generate multiple excitons that suggest that the power conversion efficiency of a solar cell could exceed 100%. However, unlike organic dye molecules that can readily infiltrate into a porous oxide film to form a self-assembled monolayer with conformal coverage on the surface of the inner pores, the infiltration of quantum dots presents a great challenge. Quantum dots have dimensions on the scale of several nanometers, in the same range as the pore size in the photoanodes, and have much smaller mobility or diffusivity. The homogeneous dispersion and uniform coverage of quantum dots inside the pore surface of photoanodes remains one of the holy grails in quantum dot-sensitized solar cells. The **Cao** group has developed a passivation strategy for ZnO mesoporous photoelectrodes for CdS/CdSe quantum dot co-sensitized solar cells (QDSCs) (**Fig. 9**). The resulting QDSCs exhibited a record power conversion efficiency (4.7%) for ZnO-based QDSCs, close to

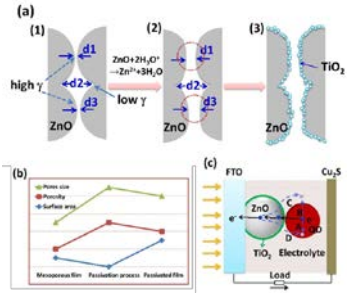

Fig. **9.** (a) Passivation process of ZnO mesoporous film, (b) variation of pores size, porosity and surface area of the film during passivation process, and (c) structure and surface charge recombination pathways of QDSC.

our similar results for TiO_2 QDSCs.[66,75] Advantages of this passivation process for QDSCs include: (1) opens pores by preferential dissolution of convex surface for homogeneous QDs distribution in the photoeletrode, (2) increases the specific surface area through deposition of TiO_2 nanoparticle layer to accommodate more QDs, and (3) suppresses the charge recombination by preventing electrons in the conduction band of ZnO from transferring to the oxidized ions in the electrolyte, which leads to a longer electron lifetime.

3.9 Charge Photogeneration in Hybric Polymer/PbS Blends. We used photoinduced absorption (PIA) spectroscopy to study charge generation in films of low band gap PbS quantum dots blended with poly(3-hexylthiophene) (P3HT) as a function of excitation energy (**Fig. 10**). Building on our previous work, we were able to selectively excite the quantum dots (or both quantum dot and polymer components) and probe the resulting long-lived excited states on the polymer by using the relatively narrow-gap P3HT host. We looked for evidence of "hot" (nonthermalized) hole transfer from photoexcited quantum dots to the conjugated polymer by measuring the yield of long-lived charge carriers in polymer/quantum dot hybrid films with varying excitation wavelength. Figure 1 shows the fractional change in probe beam transmission at the polaron peak plotted against absorbed photon flux (incident photon flux corrected by sample absorption). This gives the pump intensity-dependence of the polaron feature for the five excitation wavelengths as a function of the number of photons absorbed by the sample each second. We observe that, per photon absorbed, the yield of photogenerated holes present on the conjugated polymer increases with pump energy, even at wavelengths where only the quantum dots absorb.[86,87] We attribute this result to the transfer of nonthermalized holes from the photoexcited quantum dots to the polymer host. These results help understand the mechanisms for charge generation in hybrid organic/inorganic photovoltaics.

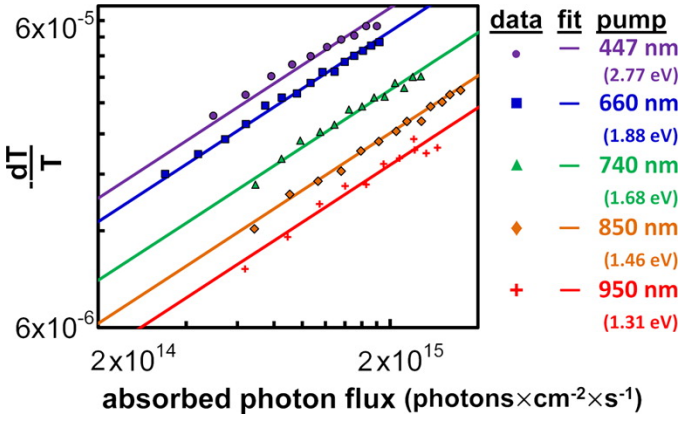

Fig. 10. Intensity dependence of the PIA polaron signal at 1050 nm (1.18 eV) for different pump energies as a function of absorbed photon flux. The straight lines are fits to the data, as explained in the text. The fit equations are as follows: $dT/T_{447} = 5.30 \times 10^{-14}(\Phi)^{0.59}$, $dT/T_{660} = 4.48 \times 10^{-14}(\Phi)^{0.59}$, $dT/T_{740} = 2.94 \times 10^{-14}(\Phi)^{0.59}$, $dT/T_{850} = 2.16 \times 10^{-14}(\Phi)^{0.59}$, and $dT/T_{950} = 1.72 \times 10^{-14}(\Phi)^{0.59}$. For clarity, we display only one data set for each pump excitation wavelength; however, the fits are best fits to the entire set of repeated measurements with each pump LED.

3.10 Highly Efficient Polymer/Polymer Bulk Heterojunction Solar Cells. We have fabricated and characterized polymer/polymer blend (all-polymer) bulk heterojunction (BHJ) solar cells with a 4.8 % power conversion efficiency (PCE) by using a thiazolothiazole-based donor polymer (PSEHTT) and a newly developed naphthalene diimide copolymer-based acceptor polymer (PNDIS-HD) (**Fig. 11a**).[83] Very high short circuit current density of 10.47 mA/cm^2 and external quantum efficiency (EQE) of 61.3 % were obtained, showing some of the best photovoltaic parameters reported to date for all-polymer solar cells. Enhanced and balanced charge transport was observed in PSEHTT:PNDIS-HD blend films processed from chlorobenzene(CB):1,2-dichlorobenzene(DCB) mixture solvent. We observed phase-separated polymer domain sizes in the tens of nanometers by AFM imaging, which could account for the

efficient charge dissociation at the polymer/polymer donor/acceptor interface. The photovoltaic performance of similarly fabricated reference PSEHTT:$PC_{61}BM$ solar cells (PCE = 3.3 %, J_{sc} = 8.46 mA/cm^2, EQE = 53.7 %, **Fig. 11c,d**) was found to be inferior to our all-polymer solar cells. Significant light harvesting by the acceptor polymer indicates that both *photoinduced hole transfer* and *photoinduced electron transfer* are important pathways in the charge photogeneration in these highly efficient all-polymer solar cells. Our results suggest that with a suitable choice of donor and acceptor semiconducting polymers and optimized device fabrication strategies, the performance of all-polymer BHJ solar cells can exceed that of the corresponding polymer/fullerene BHJ systems.

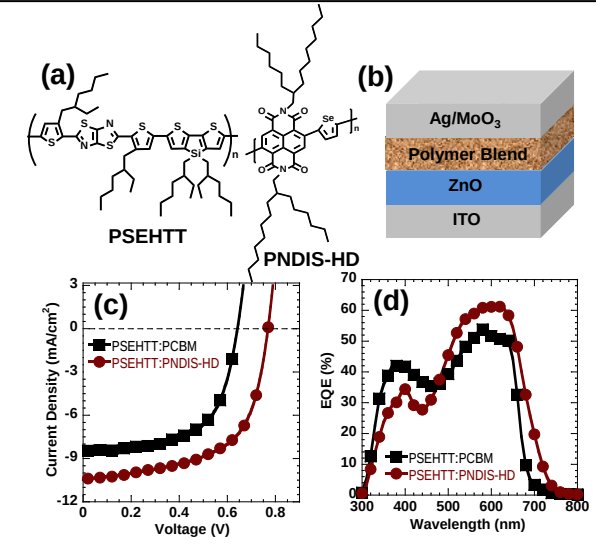

Fig. 11. (a) Molecular structures of donor (PSEHTT) and acceptor (PNDIS-HD) polymers. (b) Schematic of inverted solar cells. (c) *J–V* curves; and (d) external quantum efficiency (EQE) spectra of PSEHTT:PNDIS-HD and PSEHTT:PCBM solar cells.

3.11 Effects of ZnO-$SrTiO_3$ and ZnO-Ta_2O_5 Films as Cathodic Buffer Layers in Inverted Polymer Solar Cells. The influences of chemical composition and dielectric properties of cathodic buffer layers on power conversion efficiency in inverted polymer solar cells have been studied. Both $SrTiO_3$-ZnO and ZnO-Ta_2O_5 films with varied composition ratios were fabricated by sol-gel processing and used as the cathodic buffer layer (CBL) in inverted polymer solar cells, showing enhanced power conversion efficiency. The device performance was found to be strongly dependent on the amount of $SrTiO_3$ in the ZnO CBL. With a small amount of quasiamorphous $SrTiO_3$ added in the ZnO film, some local ordered structure with aligned TiO_6 octohedra would likely form spontaneous polarization, and induce a self-built electric field on the interface between the BHJ active layer and the CBL, which would prevent hole transport through the CBL and reduce charge recombination and result in enhanced power conversion efficiency. However, a continued increase in the amount of quasiamorphous $SrTiO_3$ in the ZnO film led to lower electron mobility. In the present study, we found that $SrTiO_3$:ZnO composition at 10:90 offered the best performance of P3HT/$PC_{61}BM$ devices and the power conversion efficiency increased from 3.58% (pure ZnO) to 4.1%, a 15% enhancement.[88]

Similar to $SrTiO_3$-ZnO films, we found that the power conversion efficiency was strongly dependent on the amount of Ta_2O_5 in the ZnO CBLs. X-ray photoelectron spectroscopy data suggested that with the presence of Ta in ZnO CBL resulted in Ta-O-Zn bonding. Moreover, some surface grain boundaries might be covered by Ta_2O_5 and resulted in less oxygen adsorbing sites, and also Ta_2O_5, with a high dielectric constant, might provide a self-built electric field on the interface between the BHJ active layer and the CBL to reduce charge recombination. A continued increase in the amount of Ta_2O_5 in ZnO film led to lower electron mobility and low crystallinity of the ZnO CBLs. The power conversion efficiency

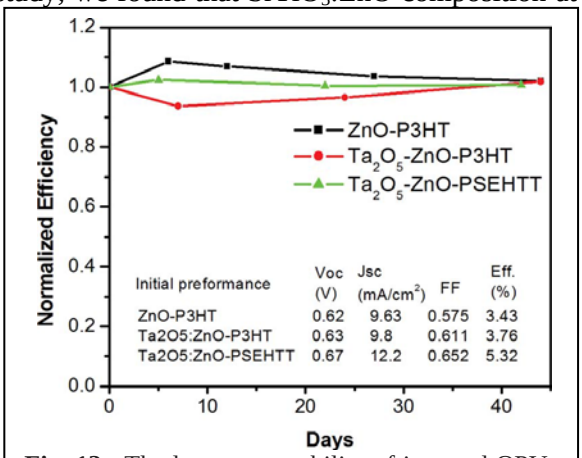

Fig. 12. The long term stability of inverted OPVs with ZnO or Ta_2O_5-ZnO films as the cathodic buffer layer; the devices were stored in ambient environment.

with P3HT/$PC_{61}BM$ system increases from 3.7% to 4.12%, an11% enhancement; in the case of PSEHTT/$PC_{71}BM$ system, from 5.29% to 5.61%. The long-term stability of unencapsulated inverted OPVs was periodically measured for 42 days, and all devices retain around 100% of their original power conversion efficiencies[89] as shown in Figure 12.

3.12 Nanostructure / Mesostructure and Performance: Scanning Probes Used to Understand Local Function. While the questions of energetics concern the ultimate theoretical limits of organic and quantum dot-based photovoltaic devices, controlling film and electrode structure on the nano- and mesoscale remains a critical practical bottleneck for these technologies. We have sought to address this problem by applying both conventional (TEM, X-ray, etc.) structural probes, as well as electrical scanning probe methods under photoexcitation that combine structural information with functional information about local carrier collection, photocurrent generation, and recombination processes. These techniques not only offer us a chance to study the effects of morphology and processing on device performance, but also to probe the fundamental operating mechanisms of hybrid bulk heterojunctions. For instance, we have used our ability to map local photocurrent collection paths using photoconductive AFM and time-resolved EFM to better understand the operating mechanism of polymer quantum dot photovoltaic blends. Previously, we believed that these blends operated primarily as bulk heterojunction devices. However, in the last funding period, we made the surprising observation that some polymer/quantum dot blends can yield high photocurrents *without* a concomitant long-lived photoinduced polaron signal.[70] Nevertheless, these polymer/quantum dot blends exhibit distinct photocurrent contributions (**Fig. 13** (top)) from both the polymer and quantum dot phases suggesting that both materials are active in light harvesting.

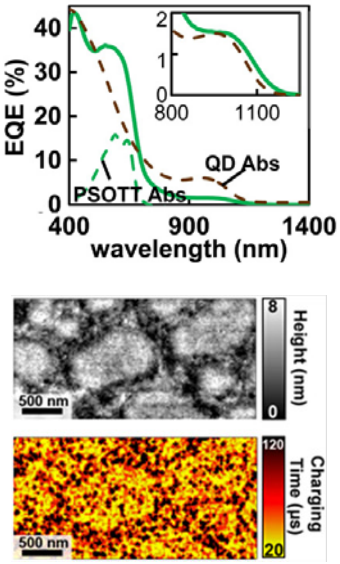

Fig. 13. (top) EQE curve for a polymer/PbS quantum dot blend that exhibits no long-lived polaron signals in PIA. We hypothesize that this blend may be operating primarily as a Schottky diode within a polymer energy transfer host. (Middle) AFM topography, and (bottom) preliminary fast trEFM charging time data (yellow is faster=better) indicating that the raised PbS domains are generating significantly photocurrent than the background, consistent with this hypothesis. (unpublished)

To explain this result, we have speculated[70] that percolating pathways of quantum dots within the polymer film may be acting as Schottky diodes that are sensitized in the visible by energy transfer from the polymer. *We propose to use high-resolution imaging of photocurrent collection to provide a direct test of this hypothesis* – if we are correct then almost all of the photocurrent will be observed in the quantum dot domains, regardless of the wavelength of the excitation light. **Fig. 13** (middle and bottom) show preliminary proof-of-concept data that this experiment should be feasible. The regions of raised topography are primarily quantum dot phases and the trEFM image shows the fastest photocharging over these regions. In the future, we plan to conduct more careful experiments with higher resolution, better signal-to-noise, and varying excitation wavelength to evaluate this hypothesis fully.

3.13 New p-Type Polymers for Excitonic Solar Cells. New materials are essential to progress in organic photovoltaics. As outlined above, some of the goals of this project were to control morphology and understand the role energetics play in recombination losses by comparing and contrasting organic and inorganic acceptors. Towards this end, we have synthesized new p-type polymers with varying HOMO/LUMO energy levels, optical bandgaps (E_g) and carrier mobilities (**Fig. 14**).[85] We have investigated the new polymers in bulk heterojunction devices with fullerene and non-fullerene inorganic and organic acceptors, characterized their morphology with conventional and scanning probe tools, and spectroscopically probed charge photogeneration in the blends. A key objective in our design of new

polymers for BHJ solar cells is achievement of mutual solubility of the materials in organic solvents along with various fullerenes or n-type polymers. In addition, we aimed to achieve large electron delocalization, efficient π–stacking and good crystallinity, tunable surface energy and wetting properties, high carrier mobility ($\mu > 10^{-3}$ cm^2/V s), optical band gaps in the 1.2-2.4 eV range, tunable HOMO/LUMO energy levels (e.g. -3.5 to -4.6 eV), and photochemical stability in air, which were achieved by some members of the series of p-type semiconducting polymers.[85]

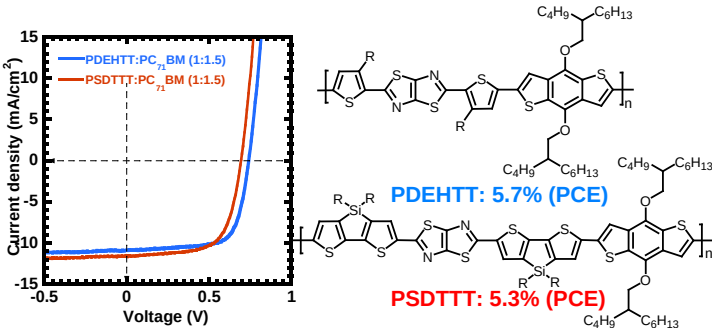

Fig. 14. J-V curves of BHJ devices containing PDEHTT and PSDTTT.

3.14 Beyond Fullerenes: Design of Non-Fullerene Acceptors for Efficient Organic Photovoltaics. Fullerene-based electron acceptors have provided the foundation for advances in fundamental understanding of charge photogeneration and practical developments in organic photovoltaics (OPVs) in the last 20 years. The power conversion efficiency (PCE) of single-junction OPV cells has steadily increased from 2.5% to current 7-9% as the donor polymer paired with a fullerene derivative has changed from poly(phenylene vinylene) derivatives to poly(3-hexylthiophene) to numerous narrow band gap copolymers. Fullerene derivatives, such as [6,6]-phenyl-C_{60}-butyric acid methyl ester ($PC_{60}BM$), have remained the most investigated electron acceptor materials in OPVs because of their overall outstanding charge photogeneration and transport properties. The prospects of enabling new pathways to OPVs while overcoming the small photovoltage, high cost, and other limitations of fullerene-based OPVs have motivated efforts to discover alternative electron acceptor materials. However, all non-fullerene acceptors reported so far have shown substantially inferior electron-accepting and photovoltaic properties in bulk heterojunction (BHJ) solar cells. Unlike the development of donor (p-type) conjugated polymers, there are as yet no general guiding principles for the design of electron acceptor (n-type) materials for OPVs.

Towards this end, recent studies have highlighted some special attributes that make fullerene derivatives such as $PC_{60}BM$ so successful as electron acceptors in OPVs: (i) the existence of low lying excited states in their monoanions, which leads to substantial enhancement in charge separation rates without affecting the charge recombination rate; (ii) their large π-conjugated molecular structure which supports efficient electronic delocalization and polaron formation; (iii) their rigid molecular architecture and high molecular diffusion that facilitate facile formation of a phase-separated nanoscale morphology for efficient charge separation and transport; and (iv) their three-dimensional (3D) spherical structure, which results in a large decrease in Coulomb barrier for charge separation due to enhanced entropic effects and enable isotropic charge transport. To date, however, non-fullerene acceptor materials are yet to be realized with a 3D molecular architecture that facilitates efficient charge photogeneration, isotropic charge transport, and photovoltaic properties comparable to the PCBMs.[82]

We have now proposed and tested a strategy for the molecular design of non-fullerene electron acceptor materials for highly efficient OPVs by adapting some of the above insights from studies of fullerene –PCBMs. The approach includes the following four main design criteria. (1) The molecule should have *an overall large, rigid, π-conjugated electron-deficient framework* that is comparable or larger than C_{60}: this is to ensure facile exciton and charge delocalization and nanometer-sized molecular objects that can mix with a donor polymer while facilitating good electron transport. (2) The molecule should have *a large density of states at the lowest unoccupied molecular orbital (LUMO)* and existence of low lying excited states of the monoanions: this is to ensure a large charge separation rate. (3) The molecule should have *a 3D non-planar architecture*: this criterion aims to avoid the efficient formation of

intermolecular exciplexes at donor/acceptor interfaces while facilitating good isotropic electron transport even in an amorphous thin film; enhanced charge separation due to entropic effects may also result. (4) The molecule should have *a multi-chromophoric architecture* such as a dimer or higher oligomer: this provides a means to enhance the density of states at the LUMO, achieve 3D non-planar conformation, and enlarge the π-conjugated framework. We have used these criteria to design and synthesize two related new π-conjugated acceptor molecules for comparison with the $PC_{60}BM$ benchmark: 8,17-diphenyl-7,9,16,18-tetraazabenzodifluoranthene-3,4,12,13-tetracarboxylic acid diimide (BFI-P2, **Fig. 15a**), which meets only criteria 1 and 2, and 2,5-bis(8-(17-phenyl)-7,9,16,18-tetraazabenzodifluoranthene-3,4,12,13-tetracarboxylic acid diimide)thiophene (DBFI-T, **Fig. 15b-c**), which meets all four criteria.

We have found that the rationally designed and experimentally realized novel, multi-chromophoric, 3D non-planar organic electron acceptor molecule, DBFI-T, outperforms $PC_{60}BM$ in both conventional and inverted OPV cells. Comparative studies of DBFI-T with its planar monomeric analogue (BFI-P2) and $PC_{60}BM$ in bulk heterojunction (BHJ) solar cells, by using a common thiazolothiazole-dithienosilole copolymer donor (PSEHTT), showed that DBFI-T has superior charge photogeneration and photovoltaic properties; PSEHTT:DBFI-T solar cells combined a high short-circuit current (10.14 mA/cm^2) with a high open-circuit voltage (0.86 V) to give a power conversion efficiency of 5.0%. The external quantum efficiency spectrum of PSEHTT:DBFI-T devices had peaks of 60–65% in the 380–620 nm range, demonstrating that both hole transfer from photoexcited DBFI-T to PSEHTT and electron transfer from photoexcited PSEHTT to DBFI-T contribute substantially to charge photogeneration. The superior charge photogeneration and electron-accepting properties of DBFI-T compared to $PC_{60}BM$ were confirmed by independent Xe-flash time-resolved microwave conductivity measurements. The π-conjugated framework of each DBFI-T molecule has a large projected planar surface area (~2×2 nm^2) for interaction with a donor polymer, which is equivalent to that of an aggregate of 9 [C_{60}]-fullerene molecules. The observed record 5% PCE along with high photocurrent, fill factor, EQE, and time-resolved microwave conductivity imply highly efficient charge photogeneration in DBFI-T/PSEHTT blends. However, the large size (surface area and volume) and largely amorphous nature of DBFI-T suggest that the detailed mechanism of charge photogeneration in DBFI-T/polymer blends may be very different from that of fullerene-PCBM/polymer systems. The multi-chromophoric 3D approach to new electron acceptors demonstrated here could be useful as a general approach in the design of more efficient OPV materials. The detailed results have been published as a full journal article.[82]

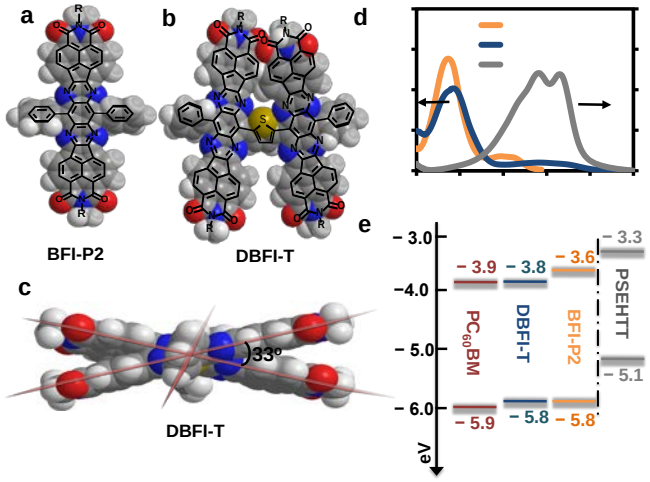

Fig. 15. The molecular structures, optical absorption spectra and energy levels of the acceptor molecules, BFI-P2 and DBFI-T. a, The molecular structure overlaid with the space filling structure of BFI-P2 after geometry optimization. **b**, The molecular structure overlaid with the space filling structure of DBFI-T after geometry optimization. **c,** Side view of the space filling structure of DBFI-T after geometry optimization. **d,** Thin film optical absorption spectra of new acceptors (BFI-P2 and DBFI-T) and donor polymer PSEHTT. **e,** Energy levels of donor polymer (PSEHTT), new non-fullerene acceptors (BFI-P2 and DBFI-T) and $PC_{60}BM$.

4. Publications Acknowledging Grant DE-FG02-07ER46467 for the Period 2007-2014.

1. Hancock, J. M.; Gifford, A. P.; Champion, R. D.; Jenekhe, S. A., Block co-oligomers for organic electronics and optoelectronics: Synthesis, photophysics, electrolurninescence, and field-effect charge transport of oligothiophene-b-oligoquinoline-b-oligothiophene triblock co-oligomers. *Macromolecules* **2008,** *41* (10), 3588-3597.
2. Xin, H.; Kim, F. S.; Jenekhe, S. A., Highly efficient solar cells based on poly(3-butylthiophene) nanowires. *J. Am. Chem. Soc.* **2008,** *130* (16), 5424-5425.
3. Xin, H.; Ren, G. Q.; Kim, F. S.; Jenekhe, S. A., Bulk Heterojunction Solar Cells from Poly(3-butylthiophene)/Fullerene Blends: In Situ Self-Assembly of Nanowires, Morphology, Charge Transport, and Photovoltaic Properties. *Chem. Mater.* **2008,** *20* (19), 6199-6207.
4. Zhang, Q. F.; Chou, T. R.; Russo, B.; Jenekhe, S. A.; Cao, G. Z., Aggregation of ZnO nanocrystallites for high conversion efficiency in dye-sensitized solar cells. *Angew. Chem. Int. Ed.* **2008,** *47* (13), 2402-2406.
5. Zhang, Q.; Chou, T. P.; Russo, B.; Jenekhe, S. A.; Cao, G., Polydisperse Aggregates of ZnO Nanocrystallites: A Method for Energy-Conversion-Efficiency Enhancement in Dye-Sensitized Solar Cells. *Adv. Funct. Mater.* **2008,** *18* (11), 1654-1660.
6. Chou, T. P.; Zhang, Q.; Russo, B.; Cao, G., Enhanced light-conversion efficiency of titanium-dioxide dye-sensitized solar cells with the addition of indium-tin-oxide and fluorine-tin-oxide nanoparticles in electrode films. *J. Nanophoton.* **2008,** *2*, 023511.
7. Wu, P.-T.; Kim, F. S.; Champion, R. D.; Jenekhe, S. A., Conjugated donor-acceptor copolymer semiconductors. synthesis, optical properties, electrochemistry, and field-effect carrier mobility of pyridopyrazine-based copolymers. *Macromolecules* **2008,** *41* (19), 7021-7028.
8. Liu, J.; Cao, G.; Yang, Z.; Wang, D.; Dubois, D.; Zhou, X.; Graff, G.; Pederson, L.; Zhang, J.-G., Oriented Nanostructures for Energy Conversion and Storage. *ChemSusChem* **2008,** *1* (8-9), 676-697.
9. Bull, T. A.; Pingree, L. S. C.; Jenekhe, S. A.; Ginger, D. S.; Luscombe, C. K., The Role of Mesoscopic PCBM Crystallites in Solvent Vapor Annealed Copolymer Solar Cells. *ACS Nano* **2009,** *3* (3), 627-636.
10. Wu, P. T.; Ren, G. Q.; Li, C. X.; Mezzenga, R.; Jenekhe, S. A., Crystalline Diblock Conjugated Copolymers: Synthesis, Self-Assembly, and Microphase Separation of Poly(3-butylthiophene)-b-poly(3-octylthiophene). *Macromolecules* **2009,** *42* (7), 2317-2320.
11. Guo, X.; Kim, F. S.; Jenekhe, S. A.; Watson, M. D., Phthalimide-Based Polymers for High Performance Organic Thin-Film Transistors. *J. Am. Chem. Soc.* **2009,** *131* (21), 7206-7207.
12. Zhang, Q. F.; Dandeneau, C.; Zhou, X. Y.; Cao, G. Z., ZnO Nanostructures for Dye-Sensitized Solar Cells. *Adv. Mater.* **2009,** *21*, 4087-4108.
13. Pingree, L. S. C.; Reid, O. G.; Ginger, D. S., Electrical Scanning Probe Microscopy on Active Organic Electronic Devices. *Adv. Mater.* **2009,** *21* (1), 19-28.
14. Noone, K. M.; Anderson, N. C.; Horwitz, N. E.; Munro, A. M.; Ginger, D. S., Absence of Photoinduced Charge Transfer in Blends of PbSe Quantum Dots and Conjugated Polymers. *ACS Nano* **2009,** *3* (6), 1345-1352.
15. Pingree, L. S. C.; Reid, O. G.; Ginger, D. S., Imaging the Evolution of Nanoscale Photocurrent Collection and Transport Networks during Annealing of Polythiophene/Fullerene Solar Cells. *Nano Lett.* **2009,** *9* (8), 2946-2952.
16. Wu, P.-T.; Bull, T.; Kim, F. S.; Luscombe, C. K.; Jenekhe, S. A., Organometallic Donor-Acceptor Conjugated Polymer Semiconductors: Tunable Optical, Electrochemical, Charge Transport, and Photovoltaic Properties. *Macromolecules* **2009,** *42* (3), 671-681.
17. Xin, H.; Guo, X. G.; Kim, F. S.; Ren, G. Q.; Watson, M. D.; Jenekhe, S. A., Efficient solar cells based on a new phthalimide-based donor-acceptor copolymer semiconductor: morphology, charge-transport, and photovoltaic properties. *J. Mater. Chem.* **2009,** *19* (30), 5303-5310.

18. Ahmed, E.; Kim, F. S.; Xin, H.; Jenekhe, S. A., Benzobisthiazole-Thiophene Copolymer Semiconductors: Synthesis, Enhanced Stability, Field-Effect Transistors, and Efficient Solar Cells. *Macromolecules* **2009,** *42* (22), 8615-8618.
19. Wu, P.-T.; Xin, H.; Kim, F. S.; Ren, G. Q.; Jenekhe, S. A., Regioregular Poly(3-pentylthiophene): Synthesis, Self-Assembly of Nanowires, High-Mobility Field-Effect Transistors, and Efficient Photovoltaic Cells. *Macromolecules* **2009,** *42* (22), 8817-8826.
20. Wu, P.-T.; Ren, G. Q.; Kim, F. S.; Li, C. X.; Mezzenga, R.; Jenekhe, S. A., Poly(3-hexylthiophene)-b-poly(3-cyclohexylthiophene): Synthesis, Microphase Separation, Thin Film Transistors, and Photovoltaic Applications. *J. Polym. Sci. A Polym. Chem.* **2010,** *48* (3), 614-626.
21. Kim, F. S.; Guo, X.; Watson, M. D.; Jenekhe, S. A. High-mobility Ambipolar Transistors and High-gain Inverters from a Donor-Acceptor Copolymer Semiconductor. *Adv. Mater.* **2010,** *22* (4), 478-482.
22. Reid, O. G.; Xin, H.; Jenekhe, S. A.; Ginger, D. S. Nanostructure Determines the Intensity-Dependence of Open-Circuit Voltage in Plastic Solar Cells. *J. Appl. Phys.* **2010,** *108* (8), 084320.
23. Wu, P.-T.; Ren, G.; Jenekhe, S. A. Crystalline Random Conjugated Copolymers with Multiple Side Chains: Tunable Intermolecular Interactions and Enhanced Charge Transport and Photovoltaic Properties. *Macromolecules* **2010,** *43* (7), 3306-3313.
24. Noone, K. M.; Strein, E.; Anderson, N. C.; Wu, P.-T.; Jenekhe, S. A.; Ginger, D. S. Broadband Absorbing Bulk Heterojunction Photovoltaics Using Low-Bandgap Solution-Processed Quantum Dots. *Nano Lett.* **2010,** *10* (7), 2635-2639.
25. Wang, C.; Kim, F. S.; Ren, G.; Xu, Y.; Pang, Y.; Jenekhe, S. A.; Jia, L. Regioregular poly(3-alkanoylthiophene): Synthesis and electrochemical, photophysical, charge transport, and photovoltaic properties. *J. Polym. Sci. A Polym. Chem.* **2010,** *48* (21), 4681-4690.
26. Yodyingyong, S.; Zhou, X.; Zhang, Q.; Triampo, D.; Xi, J.; Park, K.; Limketkai, B.; Cao, G. Enhanced Photovoltaic Performance of Nanostructured Hybrid Solar Cell Using Highly Oriented TiO2 Nanotubes. *J. Phys. Chem. C* **2010,** *114* (49), 21851-21855.
27. Chae, K.-W.; Zhang, Q. F.; Kim, J. S.; Jeong, Y. H.; Cao, G. Z. Low-Temperature Solution Growth of ZnO Nanotube Arrays. *Beilstein J. Nanotechnol.* **2010,** *1*, 128-134.
28. Park, K. S.; Zhang, Q. F.; Garcia, B. B.; Zhou, X.; Jeong, Y. H.; G. Z, C. Effect of an Ultrathin TiO2 Layer Coated on Submicrometer-Sized ZnO Nanocrystallite Aggregates by Atomic Layer Deposition on the Performance of Dye-Sensitized Solar Cells. *Adv. Mater.* **2010,** *22*, 2329-2332.
29. Zhang, Q. F.; Dandeneau, C. S.; Candelaria, S.; Liu, D. W.; Garcia, B. B.; Zhou, X. Y.; Jeong, Y. H.; Cao, G. Z. Effects of Lithium Ions on Dye-Sensitized ZnO Aggregate Solar Cells. *Chem. Mater.* **2010,** *22* (8), 2427-2433.
30. Yodyingyong, S.; Zhang, Q. F.; Park, K. S.; Dadeneau, C.; Zhou, X. Y.; Triampo, D.; Cao, G. Z., ZnO Nanoparticles and Nanowire Array Hybrid Photoanodes for Dye-sensitized Solar Cells. *Appl. Phys. Lett.* **2010,** *96*, 073115.
31. Xin, H.; Reid, O. G.; Ren, G.; Kim, F. S.; Ginger, D. S.; Jenekhe, S. A. Polymer Nanowire/Fullerene Bulk Heterojunction Solar Cells: How Nanostructure Determines Photovoltaic Properties. *ACS Nano*, **2010**, *4*, 1861–1872.
32. Ren, G.; Wu, P.-T.; Jenekhe, S. A. "Enhanced Performance of Bulk Heterojunction Solar Cells Using Block Copoly(3-alkylthiophene)s," *Chem. Mater.* **2010**, *22*, 2020-2026.
33. Zhang, Q. F.; Park, K.; Cao, G. Z. A New Microstructured DSC Photoelectrode for Potential High Power Conversion Efficiency. *J. Chin. Chem. Soc.* **2010**, *57*, 1119-1126.
34. Zhang, Q. F.; Dandeneau, C. S.; Park, K.; Liu, D. W.; Zhou, X. Y.; Jeong, Y. H.; Cao, G. Z. Light scattering with oxide nanocrystallite aggregates for dye-sensitized solar cell application. *J. Nanophotonics* **2010**, *4*, 041540-23.
35. Zhang, Q.; Park, K.; Cao, G. Synthesis of ZnO aggregates and their application in dye-sensitized solar cells. *Mater. Matters* **2010**, *5*, 32-39.
36. Ahmed, E.; Ren, G.; Kim, F. S.; Hollenbeck, E. C.; Jenekhe, S. A. Design of New Electron Acceptor Materials for Organic Photovoltaics: Synthesis, Electron Transport, Photophysics, and Photovoltaic

Properties of Oligothiophene-Functionalized Naphthalene Diimides. *Chem. Mater.* **2011,** *23* (20), 4563-4577.
37. Ahmed, E.; Subramaniyan, S.; Kim, F. S.; Xin, H.; Jenekhe, S. A. Benzobisthiazole-Based Donor-Acceptor Copolymer Semiconductors for Photovoltaic Cells and Highly Stable Field-Effect Transistors. *Macromolecules* **2011,** *44* (18), 7207-7219.
38. Noone, K. M.; Subramaniyan, S.; Zhang, Q.; Cao, G.; Jenekhe, S. A.; Ginger, D. S. Photoinduced Charge Transfer and Polaron Dynamics in Polymer and Hybrid Photovoltaic Thin Films: Organic vs Inorganic Acceptors. *J. Phys. Chem. C* **2011,** *115* (49), 24403-24410.
39. Ren, G.; Ahmed, E.; Jenekhe, S. A. Non-Fullerene Acceptor-Based Bulk Heterojunction Polymer Solar Cells: Engineering the Nanomorphology via Processing Additives. *Adv. Energy Mater.* **2011,** *1* (5), 946-953.
40. Subramaniyan, S.; Xin, H.; Kim, F. S.; Jenekhe, S. A. New Thiazolothiazole Copolymer Semiconductors for Highly Efficient Solar Cells. *Macromolecules* **2011,** *44* (16), 6245-6248.
41. Subramaniyan, S.; Xin, H.; Kim, F. S.; Shoaee, S.; Durrant, J. R.; Jenekhe, S. A. Effects of Side Chains on Thiazolothiazole-Based Copolymer Semiconductors for High Performance Solar Cells. *Adv. Energy Mater.* **2011,** *1* (5), 854-860.
42. Kim, F. S.; Ren, G.; Jenekhe, S. A. One-Dimensional Nanostructures of π-Conjugated Molecular Systems: Assembly, Properties, and Applications from Photovoltaics, Sensors, and Nanophotonics to Nanoelectronics. *Chem. Mater.* **2011,** *23* (3), 682-732.
43. Guo, X.; Xin, H.; Kim, F. S.; Liyanage, A. D. T.; Jenekhe, S. A.; Watson, M. D. Thieno[3,4-c]pyrrole-4,6-dione-Based Donor−Acceptor Conjugated Polymers for Solar Cells. *Macromolecules* **2011,** *44* (2), 269-277.
44. Park, K.; Xi, J.; Zhang, Q.; Cao, G. Charge Transport Properties of ZnO Nanorod Aggregate Photoelectrodes for DSCs. *J. Phys. Chem. C* **2011,** *115* (43), 20992-20999.
45. Park, K.; Zhang, Q.; Garcia, B. B.; Cao, G. Effect of Annealing Temperature on TiO2−ZnO Core−Shell Aggregate Photoelectrodes of Dye-Sensitized Solar Cells. *J. Phys. Chem. C* **2011,** *115* (11), 4927-4934.
46. Xi, J.; Zhang, Q.; Park, K.; Sun, Y.; Cao, G. Enhanced power conversion efficiency in dye-sensitized solar cells with TiO2 aggregates/nanocrystallites mixed photoelectrodes. *Electrochim. Acta* **2011,** *56* (5), 1960-1966.
47. Zhang, Q.; Cao, G. Nanostructured photoelectrodes for dye-sensitized solar cells. *Nano Today* **2011,** *6* (1), 91-109.
48. Bandy, J.; Zhang, Q.; Cao, G. Electrophoretic Deposition of Titanium Oxide Nanoparticle Films for Dye-Sensitized Solar Cell Applications. *Mater. Sci. Appl.* **2011,** *2*, 1427-1431.
49. Wiranwetchayan, O.; Liang, Z.; Zhang, Q. F.; Cao, G.; Singjai, P. The Role of Oxide Thin Layer in Inverted Structure Polymer Solar Cells. *Mater. Sci. Appl.* **2011,** *2*, 1697-1701.
50. Xi, J.; Zhang, Q.; Xie, S.; Yodyingyong, S.; Park, K.; Sun, Y.; Li, J.; Cao, G. Fabrication of TiO2 Aggregates by Electrospraying and Their Application in Dye-Sensitized Solar Cells. *Nanoscience and Nanotechnology Letters* **2011,** *3* (5), 690-696.
51. Zhang, Q.; Cao, G. Hierarchically structured photoelectrodes for dye-sensitized solar cells. *J. Mater. Chem.* **2011,** *21* (19), 6769-6774.
52. Zhang, Q.; Park, K.; Xi, J.; Myers, D.; Cao, G. Recent Progress in Dye-Sensitized Solar Cells Using Nanocrystallite Aggregates. *Adv. Energy Mater.* **2011,** *1* (6), 988-1001.
53. Giridharagopal, R.; Rayermann, G. E.; Shao, G.; Moore, D. T.; Reid, O. G.; Tillack, A. F.; Masiello, D. J.; Ginger, D. S. "Submicrosecond Time Resolution Atomic Force Microscopy for Probing Nanoscale Dynamics," *Nano Lett.* **2012**, *12*, 893-898.
54. Hwang, Y. –J.; Ren, G.; Murari, N. M.; Jenekhe, S. A. "n-Type Naphthalene Diimide-Biselenophene Copolymer for All-Polymer Bulk Heterojunction Solar Cells," Macromolecules **2012**, 45, 9056-9062.
55. Ren, G.; Ahmed, E.; Jenekhe, S. A. "Nanowires of Oligothiophene-functionalized Naphthalene Diimides: Self Assembly, Morphology, and All-Nanowire Bulk Heterojunction Solar Cells," *J. Mater. Chem.* **2012**, *22*, 24373-24379.

56. Zhang, Q.; Myers, D.; Lan, J.; Jenekhe, S. A.; Cao G. Z. “Application of Light Scattering in Dye-Sensitized Solar Cells,” *Phys. Chem. Chem. Phys.* **2012**, *14*, 14982-14998.
57. Xin, H.; Subramaniyan, S.; Kwon, T.-W.; Shoaee, S.; Durrant, J. R.; Jenekhe, S. A. “Enhanced Open Circuit Voltage and Efficiency of Donor-Acceptor Copolymer Solar Cells by Using Indene-C60 Bisadduct,” *Chem. Mater.***2012**, *24*, 1995-2001.
58. Xin, H.; Guo, X.; Ren, G.; Watson, M. D.; Jenekhe, S. A. “Efficient Phthalamide Copolymer-Based Bulk Heterojunction Solar Cells: How the Processing Additive Influences Nanoscale Morphology and Photovoltaic Properties,” *Adv. Energy Mater.* **2012**, *2*, 575-582.
59. Zhang, Q. F.; Yodyingyong, S.; Xi, J. T.; Myers, D.; Cao, G. Z. Oxide nanowires for solar cell applications. *Nanoscale* **2012**, *4*, 1436-1445.
60. Subramaniyan, S.; Kim, F. S.; Ren, G.; Li, H.; Jenekhe, S. A. “High Mobility Thiazole−Diketopyrrolopyrrole Copolymer Semiconductors for High Performance Field-Effect Transistors and Photovoltaic Devices,” *Macromolecules* **2012**, *45*, 9029-9037.
61. Yang, Z.; Zhang, Q. F.; Xi, J. T.; Park, K.; Xu, X. L.; Liang, Z. Q.; Cao, G. Z. CdS/CdSe Co-Sensitized Solar Cell Prepared by Jointly Using Successive Ion Layer Absorption and Reaction Method and Chemical Bath Deposition Process. *Sci. Adv. Mater.* **2012**, *4*, 1013-1017.
62. Xi, J. T.; Zhang, Q. F.; Myers, D.; Sun, Y. M.; Cao, G. Z. Hollow hemispherical titanium dioxide aggregates fabricated by coaxial electrospray for dye-sensitized solar cell application. *J. Nanophotonics* **2012**, *6*, 063519-11.
63. Xi, J. T.; Wiranwetchayan, O.; Zhang, Q. F.; Liang, Z. Q.; Sun, Y. M.; Cao, G. Z. Growth of single-crystalline rutile TiO_2 nanorods on fluorine-doped tin oxide glass for organic-inorganic hybrid solar cells. *J. Mater. Sci.*: *Mater. Electron.* **2012**, *23*, 1657-1663.
64. Xi, J. T.; Al Dahoudi, N.; Zhang, Q. F.; Sun, Y. M.; Cao, G. Z. Effect of Annealing Temperature on the Performances and Electrochemical Properties of TiO_2 Dye-Sensitized Solar Cells. *Sci. Adv. Mater.* **2012**, *4*, 727-733.
65. Wiranwetchayan, O.; Zhang, Q. F.; Zhou, X. Y.; Liang, Z. Q.; Singjai, P. Cao, G. Z. Impact of the Morphology of TiO2 Films as cathode Buffer Layer on the Efficiency of Inverted-Strcuture Polymer Solar Cells. *Chalcogenide Lett.* **2012**, *9*, 157-163.
66. Tian, J. J.; Gao, R.; Zhang, Q. F.; Zhang, S. G.; Li, Y. W.; Lan, J. L.; Qu, X. H.; Cao, G. Z. Enhanced Performance of CdS/CdSe Quantum Dot Cosensitized Solar Cells via Homogeneous Distribution of Quantum Dots in TiO_2 Film. *J. Phys. Chem. C* **2012**, *116*, 18655-18662.
67. Liang, Z. Q.; Zhang, Q. F.; Wiranwetchayan, O. ; Xi, J. T.; Yang, Z.; Park, K.; Li, C. D.; Cao, G. Z. Effects of the Morphology of a ZnO Buffer Layer on the Photovoltaic Performance of Inverted Polymer Solar Cells. *Adv. Funct. Mater.* **2012**, *22*, 2194-2201.
68. Al Dahoudi, N. ; Zhang, Q. F.; Cao, G. Z. Alumina and Hafnia ALD Layers for a Niobium-Doped Titanium Oxide Photoanode. *Intl. J. Photoenergy* **2012**, 401393-6.
69. Colbert, A. E.; Janke, E. M.; Hsieh, S. T.; Subramaniyan, S.; Schlenker, C. W.; Jenekhe, S. A.; Ginger, D. S. “Hole Transfer from Low Band Gap Quantum Dots to Conjugated Polymers in Organic/Inorganic Hybrid Photovoltaics,” *J. Phys. Chem. Lett.* **2013**, *4*, 280-284.
70. Strein, E.; Colbert, A.; Subramaniyan, S.; Nagaoka, H.; Schlenker, C. W.; Janke, E.; Jenekhe, S. A.; Ginger, D. S. “Charge generation and energy transfer in hybrid polymer/infrared quantum dot solar cells,” *Energy Environ. Sci.* **2013**, *6*, 769-775.
71. Ren, G.; Schlenker, C. W.; Ahmed, E.; Subramaniyan, S.; Olthof, S.; Kahn, A.; Ginger, D. S.; Jenekhe, S. A. “Photoinduced Hole Transfer Becomes Suppressed with Diminished Driving Force in Polymer-Fullerene Solar Cells While Electron Transfer Remains Active,” *Adv. Funct. Mater.* **2013**, *23*, 1238-1249.
72. Earmme, T.; Hwang, Y.-J.; Murari, N. M.; Subramaniyan, S.; Jenekhe, S. A. All-Polymer Solar Cells with 3.3% Efficiency Based on Naphthalene Diimide-Selenophene Copolymer Acceptor. . *J. Am. Chem. Soc.*, **2013**, *135*, 14960–14963.

73. Richards, J. J.; Rice, A. H.; Nelson, R. D.; Kim, F. S.; Jenekhe, S. A.; Luscombe, C. K.; Pozzo, D. C. Modification of PCBM Crystallization via Incorporation of C_{60} in Polymer/Fullerene Solar Cells. *Adv. Funct. Mater*. **2013**, *23*, 514–522.
74. Zhang, Q. F.; Uchaker, E.; Candelaria, S. L.; Cao, G. Z. Nanomaterials for energy conversion and storage. *Chem. Soc. Rev.* **2013**, *42*, 3127-3171.
75. Tian, J. J.; Zhang, Q. F.; Zhang, L. L.; Gao, R.; Shen, L. F.; Zhang, S. G.; Qu, X. H.; Cao, G. Z. ZnO/TiO_2 nanocable structured photoelectrodes for CdS/CdSe quantum dot co-sensitized solar cells. *Nanoscale* **2013**, *5*, 936-943.
76. Tian, J. J.; Zhang, Q. F.; Uchaker, E.; Gao, R.; Qu, X. H.; Zhang, S. E.; Cao, G. Z. Architectured ZnO photoelectrode for high efficiency quantum dot sensitized solar cells. *Energy Environ. Sci*. **2013**, *6*, 3542-3547.
77. Park, K.; Zhang, Q. F.; Myers, D.; Cao, G. Z. Charge Transport Properties in TiO_2 Network with Different Particle Sizes for Dye Sensitized Solar Cells. *ACS Appl. Mater. Interfaces* **2013**, *5*, 1044-1052.
78. Gao, R.; Tian, J. J.; Liang, Z. Q.; Zhang, Q. F.; Wang, L. D.; Cao, G. Z. Nanorod-nanosheet hierarchically structured ZnO crystals on zinc foil as flexible photoanodes for dye-sensitized solar cells. *Nanoscale* **2013**, *5*, 1894-1901.
79. Gao, R.; Liang, Z. Q.; Tian, J. J.; Zhang, L. D. Wang and G. Z. Cao. ZnO nanocrystallite aggregates synthesized through interface precipitation for dye-sensitized solar cells. *Nano Energy* **2013**, *2*, 40-48.
80. Gao, R.; Liang, Z. Q.; Tian, J. J.; Zhang, Q. F.; Wang L. D.; Cao, G. Z. A ZnO nanorod layer . with a superior light-scattering effect for dye-sensitized solar cells. *RSC Adv.* **2013**, *3*, 18537-18543.
81. Al Dahoudi, Zhang, N.; Cao, G. Z. Low-Temperature Processing of Titanium Oxide Nanoparticles Photoanodes for Dye-Sensitized Solar Cells. *J. Renew. Energy* **2013**, 545212-20.
82. Li, H.; Earmme, T.; Ren, G.; Saeki, A.; Yoshikawa, S.; Murari, N. M.; Subramaniyan, S.; Crane, M. J.; Seki, S.; Jenekhe, S. A. "Beyond Fullerenes: Design of Nonfullerene Acceptors for Efficient Organic Photovoltaics," *J. Am. Chem. Soc.* **2014**, *136*, 14589-14597.
83. Earmme, T.; Hwang, Y.-J.; Subramaniyan, S.; Jenekhe, S. A. "All-Polymer Bulk Heterojunction Solar Cells with 4.8% Efficiency Achieved by Solution Processing from a Co-Solvent," *Adv. Mater*. **2014**, *26*, 6080-6085.
84. Murari, N. M.; Crane, M. J.; Earmme, T.; Hwang, Y. –J.; Jenekhe, S. A. "Annealing Temperature Dependence of the Efficiency and Vertical Phase Segregation of Polymer/Polymer Bulk Heterojunction Photovoltaic Cells," *Appl. Phys. Lett.* **2014**, *104*, 223906.
85. Subramaniyan, S.; Xin, H.; Kim, F. S.; Murari, N. M.; Courtright, B. A. E.; Jenekhe, S. A. "Thiazolothiazole Donor-Acceptor Conjugated Polymer Semiconductors for Photovoltaic Applications," *Macromolecules,* **2014**, *47*, 4199-4209.
86. Strein, E.; de Quilettes, D. W.; Hsieh, S. T.; Colbert, A. E.; Ginger, D. S. "Hot Hole Transfer Increasing Polaron Yields in Hybrid Conjugated Polymer/PbS Blends," *J. Phys. Chem. Lett.* **2014**, *5*, 208-211.
87. Nagaoka, H.; Colbert, A. E.; Strein, E.; Janke, E. M.; Salvador, M.; Schlenker, C. W.; Ginger, D. S. "Size-Dependent Charge Transfer Yields in Conjuaged Polymer/Quantum Dot Blends," *J. Phys. Chem. C* **2014**, *118*, 5710-5715.
88. Lan, J. –L.; Cherng, S.-J.; Yang, Y.-H.; Zhang, Q.; Subramaniyan, S.; Ohuchi, F. S.; Jenekhe, S. A.; Cao, G. "The effects of Ta_2O_5-ZnO films as cathodic buffer layers in inverted polymer solar cells," *J. Mater. Chem. A* **2014**, *2*, 9361-9370.
89. Lan, J. –L.; Liang, Z.; Yang, Y. H.; Ohuchi, F. S.; Jenekhe, S. A.; Cao, G. Z. "The Effect of SrTiO3:ZnO as Cathodic Buffer Layer for Inverted Polymer Solar Cells," *Nano Energy* **2014**, *4*, 140-149.
90. Gao, R.; Cui, Y.X.; Liu, X.J.; Wang, L.D.; Cao, G. Z., "A ZnO nanorod/nanoparticle hierarchical structure synthesized through a facile in situ method for dye-sensitized solar cells," *J. Mater. Chem. A* **2014**, 2, 4765–4770.

5. Project Personnel

5a. Postdoctoral Research Associates/Scientists:

Dr. Hao Xin – 50 % support, 2007-2012.
Dr. Selvam Subramaniyan – 50 % support, 2008-2009.
Dr. Abhishek Kulkarni – 42 % support, 2008-2010.
Dr. Jeff Zhang – 25 % support, 2007-2014.
Dr. Sarah Zhou – 50 % support, 2007-2012.
Dr. Liam Pingree – 0% salary, materials only, 2007-2009(funded by NSF Discovery Corps Fellowship).
Dr. Cody Schlenker – 5% support, 2012-2013 (95% funding by NSF fellowship)
Dr. Jolin Lan – 50 % support, 2013-2014.

5b. PhD Graduate Students:

Felix Kim – 50% support, 2008-2013.
Guoquain Ren – 50% support, 2011-2013.
Taeshik Earmme – 40% support, 2013-2014.
Obadiah Reid – 0% salary, materials only 2008-2009 (salary funded on NSF IGERT fellowship).
Kevin Noone – 50% support, 2008-2012.
Marsha Ng – PhD Student, 50% support.
Adam Colbert – 50% support, 2012-2014.
Kwangsuk Park – 25% support, 2007-2011.
Christopher Dandeneau – 20% support, 2007-2009.

5c. Undegraduate Students:

Eric Janke – 0% support, materials and facility user fees.
Jason Bandy – 0% support, materials and facility user fees; worked on the project for his senior thesis.

5d. Visiting Scholars/Scientists/ Students (0% Salary, materials and facility user fees only):

Dr. Hirokazu Nagaoka – (2011-2013): supported with Japanese funding.
Dr. Jianjun Tian – (2011-2012): supported by home institution funding.
Junting Xi – (2009-2011): worked on the project but funded by her full scholarship.
Orawan Wiranwetchayan – (2010-2011): worked on the project but funded by her full scholarship.
Zhou Yang – (2010-2011): worked on the project but funded by his full scholarship.
Zhiqiang Liang – (2010-2012): worked on the project but funded by his full scholarship.